

EMA-Net: Efficient Multitask Affinity Learning for Dense Scene Predictions

Dimitrios Sinodinos^{1,2}, Narges Armanfard^{1,2}

¹McGill University

²Mila Quebec

dimitrios.sinodinos@mail.mcgill.ca, narges.armanfard@mcgill.ca

Abstract

Multitask learning (MTL) has gained prominence for its ability to jointly predict multiple tasks, achieving better per-task performance while using fewer per-task model parameters than single-task learning. More recently, decoder-focused architectures have considerably improved multitask performance by refining task predictions using the features of other related tasks. However, most of these refinement methods fail to simultaneously capture local and global task-specific representations, as well as cross-task patterns in a parameter-efficient manner. In this paper, we introduce the Efficient Multitask Affinity Learning Network (EMA-Net), which is a lightweight framework that enhances the task refinement capabilities of multitask networks. EMA-Net adeptly captures local, global, and cross-task interactions using our novel Cross-Task Affinity Learning (CTAL) module. The key innovation of CTAL lies in its ability to manipulate task affinity matrices in a manner that is optimally suited to apply parameter-efficient grouped convolutions without worrying about information loss. Our results show that we achieve state-of-the-art MTL performance for CNN-based decoder-focused models while using substantially fewer model parameters. Our code is publicly available at <https://github.com/Armanfard-Lab/EMA-Net>.

1 Introduction

Modern AI research is rapidly integrating into our daily lives. However, most cutting-edge models are massive and rely on remote access since they cannot be easily deployed on edge devices such as mobile phones, smart accessories, or wearable medical equipment. For many applications, the need for models to operate locally without network dependence highlights the importance of balancing performance with parameter efficiency in model design.

In recent years, multitask learning (MTL) [Caruana, 1997] has emerged as a parameter-efficient learning paradigm that can also outperform traditional single-task learning (STL). Generally, MTL involves a single network that can learn multiple tasks by jointly optimizing multiple loss functions. Con-

sequently, using a single network means that several layers or features are being shared between tasks. In many dense prediction cases, sharing features across tasks has been proven to improve per-task performance, while using fewer per-task model parameters. This is the result of improved generalization by leveraging domain-specific knowledge between related tasks [Kendall *et al.*, 2018]. The prominent research directions for modern MTL methods explore either the optimization strategy [Chen *et al.*, 2018; Liu *et al.*, 2022; Xin *et al.*, 2022] or the design of the deep multitask architecture [Misra *et al.*, 2016; Gao *et al.*, 2019; Sinodinos and Armanfard, 2022]. Within the vein of deep architecture design, Vandenhende *et al.* [2022] further fragment the designs into encoder-focused and decoder-focused architectures. As the name suggests, decoder-focused models employ feature-sharing mechanisms within the decoder(s). Specifically, decoder-focused architectures introduce mechanisms to refine task predictions by capturing feature patterns between tasks. An example of a pattern between tasks would be the alignment of segmentation edges with discontinuities in depth values. This refinement process is also called task prediction distillation [Xu *et al.*, 2018]. By capturing these inter-task relationships, decoder-focused architectures consistently achieve state-of-the-art performance in MTL and can be regarded as the prevailing research direction for multitask architecture design.

A foundational decoder-focused method, PAP-Net [Zhang *et al.*, 2019], introduces the notion of “task affinity”, which is a measure of similarity between pairs of features for a given task. Specifically, they construct affinity matrices to store the similarity information between every possible pair of features for a given task. The benefit of working with affinity matrices is that they capture long-range dependencies and introduce very few additional model parameters. To perform task prediction distillation, they combine affinity matrices from all tasks using a weighted sum, and then diffuse this similarity information into the features of each initial task prediction. A problem with this approach is that learning a single weight per affinity matrix suggests that all pairwise similarity patterns in the feature space are equally important. However, we hypothesize that cross-task patterns are nuanced and vary in importance throughout the feature space. This simple cross-task mechanism was likely used because processing these matrices can be expensive, especially at larger feature

scales. Grounded by our hypothesis, we believe that **there is substantial untapped potential in affinity representations (i)**.

A more recent work, MTI-Net [Vandenhende *et al.*, 2020], claims that tasks with high affinities at a certain feature scale are not guaranteed to have high affinities at different scales. Consequently, they model task interactions at multiple scales to perform “multi-scale multi-modal distillation”; which significantly improves performance. However, this performance improvement comes at the cost of additional parameters for deep supervision at multiple scales; which makes this approach susceptible to overfitting on simpler datasets. Therefore, we believe that **there is a need for a more parameter-efficient framework that can still leverage the benefits of multiscale processing (ii)**.

InvPT [Ye and Xu, 2022] and TaskPrompter [Ye and Xu, 2023] continue the trend of improving performance with more model capacity by moving away from the CNN architecture for one based on the Vision Transformer (ViT) [Dosovitskiy *et al.*, 2020]. They argue that current multitask attention mechanisms in CNN-based models have limited scope in their cross-task pattern modelling. Their multitask attention methods can capture local, global, and cross-task relationships, but mainly because they operate on more compressed features as a consequence of using feature extractors with significantly higher parameter budgets. However, **modelling local, global, and cross-task relationships has yet to be accomplished using lightweight CNN-based feature extractors (iii)**.

Despite their recent success, current decoder-focused methods have yet to address (i), (ii), and (iii). We solve all of these issues by introducing the Efficient Multitask Affinity Learning Network (EMA-Net), which uses our novel Cross-Task Affinity Learning (CTAL) module for improved task prediction distillation. CTAL strategically aligns the affinity matrices using careful reshaping and interleaved concatenations, which allows us to leverage grouped convolutions to realize massive reductions in model parameters. Additionally, since we exhaustively model every pairwise feature relationship within a task and across all tasks, we can use these grouped convolutions without fear of information loss. This effectively solves issue (i), as we can tap into the full potential of affinity matrix representations. Simultaneously, we also solve issue (iii), since our cross-task attention mechanism explicitly models all pairwise interactions intra- and inter-task using only a lightweight CNN-based architecture. Our method also extends to a multiscale framework by applying deep supervision to initial task predictions at multiple scales. However, unlike MTI-Net, we fuse the initial task predictions from every scale and then perform task prediction distillation at a single scale. Consequently, our multi-scale EMA-Net framework is more parameter efficient, and addresses issue (ii). Therefore, we can summarize our contributions as follows:

1. A method to process affinity matrices in a parameter-efficient manner while exhaustively modelling all intra- and inter-task relationships in CNN-based architectures. This addresses (i, iii).

2. A light-weight multiscale framework that yields the benefits of multiscale deep supervision, while only needing a single scale for task-prediction distillation. This addresses (ii).

As a result of our contributions, we achieve significant multi-task performance improvements using a fraction of the learnable parameters compared to other decoder-focused techniques.

2 Related Works

PAD-Net [Xu *et al.*, 2018] is the first work to popularize the idea of refining task predictions by distilling their feature information between tasks. They refer to this process as “task prediction distillation”. PAP-Net [Zhang *et al.*, 2019] explicitly models feature similarities, known as “task affinity”, and distills this information between tasks. MTI-Net [Vandenhende *et al.*, 2020] extends distillation to multiple feature scales, which is known as “multi-scale multi-modal” distillation. Other recent works include ATRC [Brüggenmann *et al.*, 2021], InvPt [Ye and Xu, 2022], and TaskPrompter [Ye and Xu, 2023]. ATRC applies a neural architecture search (NAS) to learn a branching structure that considers the global features, local features, source label, and target labels between every possible combination of task pairs. Although this study provides interesting insights into optimal task interactions, it is difficult to justify its use in a real-world setting because it takes an incredible amount of resources to train, and scales very poorly with more tasks. Hanrong Ye and Dan Xu [2022; 2023] create their own multitask network based on the Vision Transformer (ViT) [Dosovitskiy *et al.*, 2020]. The added model capacity allows them to explicitly model local and global relationships between tasks.

The attention mechanism [Vaswani *et al.*, 2017] allows networks to place greater emphasis on certain parts of an input that are important for the downstream task. For dense vision tasks, it has been shown that attending to features in the spatial and/or channel dimensions leads to significant performance improvements [Woo *et al.*, 2018; Fu *et al.*, 2019]. Consequently, these notions have been extended to the MTL domain, which explored different ways of modelling cross-task patterns using attention [Liu *et al.*, 2019; Xu *et al.*, 2018; Zhang *et al.*, 2019; Vandenhende *et al.*, 2020; Sinodinos and Armanfard, 2022].

3 EMA-Net

In the literature, there are two prevailing approaches to applying an attention map to a set of image features generated by CNN-based architectures. The first approach involves using convolutional blocks to process the features and obtain an attention mask with the same shape. The attention mask undergoes an activation (i.e., Sigmoid) to set all values to be between 0 and 1. The resulting attention map is applied to the features via element-wise multiplication, which has been applied in STL [Woo *et al.*, 2018], and MTL [Liu *et al.*, 2019; Xu *et al.*, 2018]. We will refer to this as element-wise multiplication attention (EM attention). The second approach aims to explicitly model long-range dependencies of features by computing the Gram matrix (inner products of all pairs of

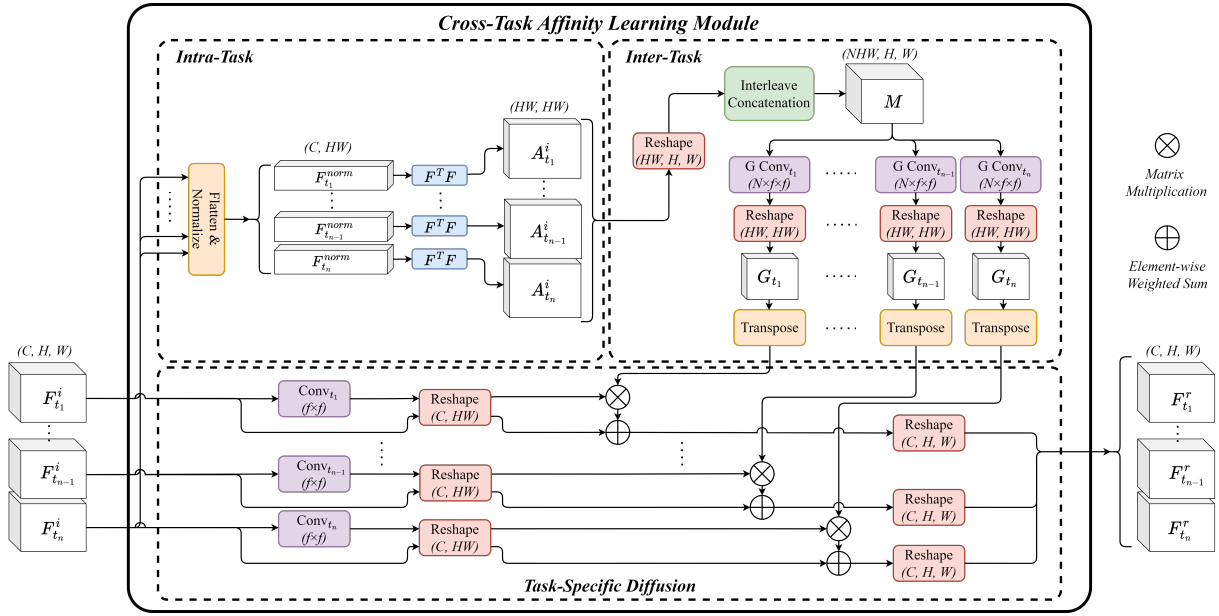


Figure 1: A diagram of the Cross-Task Affinity Learning (CTAL) module that is comprised of three stages: Intra-Task, Inter-Task, and Task-Specific Diffusion. We compute the Gram matrix of the flattened and normalized views of the initial task prediction features $F_{t_k}^i$ to obtain the task-specific affinity matrices $A_{t_k}^i$. We then reshape $A_{t_k}^i$ to the original spatial dimensions and perform an interleaved concatenation of all HW channels for each task to obtain the joint affinity matrix M . Each of the HW sets of N channels is processed by a task-specific grouped convolution ($G \text{ Conv}_{t_k}$) and then diffuses its information to a projected view of $F_{t_k}^i$ via matrix multiplication and an element-wise weighted sum to obtain the final refined features $F_{t_k}^r$.

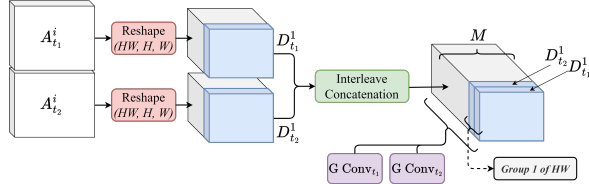


Figure 2: An illustration of the interleave concatenation procedure used to align the channels for grouped convolutions in a two-task scenario.

column vectors) of the features after flattening them along the spatial dimensions. The corresponding matrix (i.e., affinity matrix) is then diffused to the original features via matrix multiplication. We will refer to this method as matrix multiplication attention (MM attention). MM attention has also been used in STL [Fu *et al.*, 2019], and MTL [Zhang *et al.*, 2019]. In MTL, the EM attention from PAD-Net and the MM attention from PAP-Net achieve almost identical results. However, PAP-Net uses considerably fewer model parameters at the cost of more floating point operations (FLOPs). Their comparable performance is likely attributed to the fact that the affinity matrices explicitly capture long-range dependencies between every feature pair and diffuse them across all features using MM attention; whereas EM attention approaches only learn long-range dependencies implicitly by training convolutional filters that process local patches throughout the entire spatial dimension.

The fact that MM attention in PAP-Net achieves al-

most identical performance to EM attention using a simple weighted sum for cross-task fusion is astonishing. We believe that there is substantial untapped potential in these affinity representations, and therefore, we were inspired to develop a parameter-efficient cross-task attention mechanism to optimally model local and global interactions. For parameter efficiency, we aim to employ MM attention, which involves processing large affinity matrices. Therefore the challenge lies in minimizing the parameters introduced to process these matrices. We propose our EMA-Net framework to efficiently and exhaustively model all cross-task patterns using CTAL; which is comprised of three stages: intra-task modelling, inter-task modelling, and task-specific diffusion.

3.1 Intra-Task Modelling

As seen in Figure 1, for a given task $t_k \{k \in [1, N]\}$, we follow the standard procedure to generate the affinity matrices, $A_{t_k} \in \mathbb{R}^{HW, HW}$. This involves taking the features of the initial predictions, $F_{t_k} \in \mathbb{R}^{C, H, W}$, flattening the spatial dimensions, performing L2 normalization for each column, and computing the Gram matrix (the inner products of all pairs of column vectors). At this point, every row in A_{t_k} contains the cosine similarities of a feature, $x \in F_{t_k}$, with every other feature in F_{t_k} . Next, we reshape A_{t_k} into $\mathbb{R}^{HW, H, W}$. This restores the original spatial dimensions of the features, but now the HW channels at a given 2-dimensional position ($i \in [1, H], j \in [1, W]$) contain the cosine similarities of the feature $x_{i,j}$ with all other features. Therefore, in this configuration, the entire first channel corresponds to the similarities of all $x_{i,j}$ with $x_{1,1}$, which is also aligned at position (i, j) .

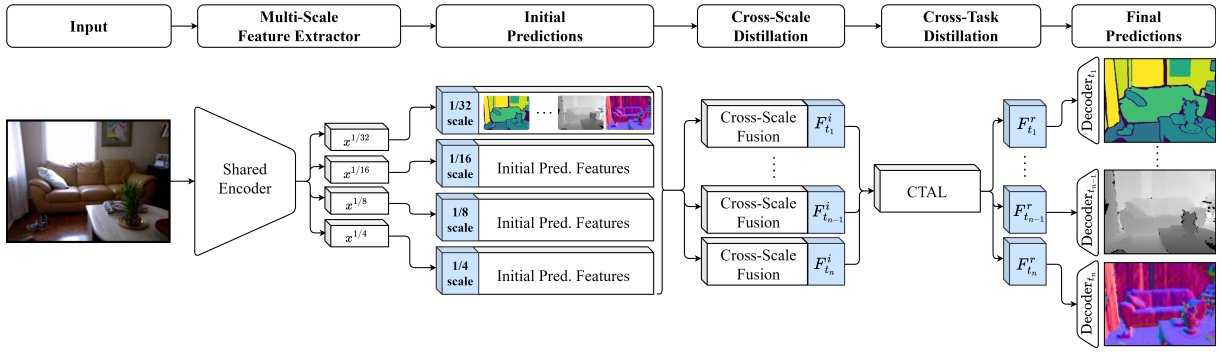


Figure 3: A network diagram of EMA-Net using deep supervision at multiple feature scales and using the CTAL module after cross-scale fusion for task-refinement. An input image is passed through a shared encoder to generate a set of features at 4 different scales relative to the input. We compute the initial predictions using each feature scale and then upsample all task-specific feature maps to the highest scale and combine them in the cross-scale fusion blocks. Finally, the output of each task-specific cross-scale fusion is passed as input to the CTAL module, where the features are refined and then processed by task-specific decoders to obtain the final predictions.

This is a useful property for maintaining spatial coherence during subsequent processing.

3.2 Inter-Task Modelling

Next, to fuse the reshaped affinity matrices, we first perform an interleaved concatenation operation. As seen in Figure 2, this involves concatenating the first channel of each \mathbf{A}_{t_k} (i.e. $D_{t_1}^1$ and $D_{t_2}^1$), and then the second channels, and so on for all HW channels of each \mathbf{A}_{t_k} . This gives us the joint affinity matrix, $\mathbf{M} \in \mathbb{R}^{NHW, HW}$, where N is the number of tasks in the MTL system. Depending on the spatial dimensions of the data, this \mathbf{M} can be very large, so processing it using standard convolutions would be very expensive. Instead, we aim to leverage parameter-efficient grouped convolutions [Xie *et al.*, 2017; Chollet, 2017; Sandler *et al.*, 2018]. The way we strategically organized \mathbf{M} strongly justifies the use of grouped convolutions to perform our multitask fusion without the fear of losing important cross-task information. This is because every group of N channels already contains task interactions between a given feature $x_{i,j}$ with every other feature across all tasks. So not only does this significantly reduce the number of model parameters required to fuse \mathbf{M} for every task, but it also allows us to learn HW spatially coherent kernels that specifically focus on learning the relationships of a given feature $x_{i,j}$ with all other features across all tasks. When considering a traditional convolution on \mathbf{M} , we would require HW kernels of size $NHW \times f \times f$, whereas our approach only requires HW kernels of size $N \times f \times f$, where f is the size of the convolutional filter. This translates to HW times fewer parameters used. For example, working with 3 tasks at 72×96 feature size and $f = 3$, for the NYUv2 dataset, we use only 187K parameters compared to the 1.29B parameters needed for a single standard convolutional layer.

After processing the shared \mathbf{M} for every task, we obtain N matrices and reshape each of them back into $HW \times HW$ to obtain each $\mathbf{G}_{t_k} \in \mathbb{R}^{HW, HW}$. Now, in a given \mathbf{G}_{t_k} , each row contains information about the relationship of a single feature with every other feature across all tasks. Since we use $f \times f$ kernels where $f > 1$, we also embed cross-task spatial interaction patterns. Next, we transpose the matrix

so that the row containing all pertinent information for $x_{i,j}$ is stored at location (i, j) after the diffusion process, which perfectly maintains spatial coherence throughout the entire attention process.

3.3 Task-Specific Diffusion

The subsequent diffusion process involves performing a matrix multiplication to obtain the diffused features, $\mathbf{F}_{t_k}^d \in \mathbb{R}^{C, HW}$:

$$\mathbf{F}_{t_k}^d = \mathbf{F}_{t_k}^p \times \mathbf{G}_{t_k}^\top, \quad (1)$$

where $\mathbf{F}_{t_k}^p \in \mathbb{R}^{C, HW}$ is the reshaped convolution projection of $\mathbf{F}_{t_k}^i$. Through this matrix multiplication, every value in $\mathbf{F}_{t_k}^d$ is the result of the dot product between a row vector in $\mathbf{F}_{t_k}^p$ containing values from all HW features and a column vector in $\mathbf{G}_{t_k}^\top$ containing cross-task affinity pattern information between a feature $x_{i,j}$ and all other HW features. When there is a high-affinity pattern across tasks, the value of $x_{i,j}$ will become larger relative to other features with lower-affinity patterns, similar to the scaling behaviour from EM attention. As seen in Equation 2, the diffused features are then blended with the original features using element-wise addition with scalar weighing parameter γ to obtain the refined features $\mathbf{F}_{t_k}^r \in \mathbb{R}^{C, HW}$. This blending ensures the refined features do not deviate too far from the original features.

$$\mathbf{F}_{t_k}^r = \gamma * \mathbf{F}_{t_k}^d + (1 - \gamma) * \mathbf{F}_{t_k}^i \quad (2)$$

3.4 Multiscale EMA-Net

There are two variants of the proposed EMA-Net architecture. The first variant makes initial predictions using a single feature scale (SS) and the other using multiple feature scales (MS). The latter is illustrated in Figure 3, which is used to compete with multi-scale multi-modal distillation methods like MTI-Net [Vandenhende *et al.*, 2020]. However, our model is more efficient and scalable as we only need a single distillation module (i.e. CTAL) rather than having one module for every scale. We accomplish this by combining

the initial prediction features from each scale with the cross-scale fusion (CSF) blocks prior to performing task prediction distillation in CTAL. For cross-scale fusion, we follow the same procedure as [Vandenhende *et al.*, 2020], which involves up-sampling all features to the 1/4 input scale, concatenating them along the channel dimension, and combining them through a convolutional block. For comparison with other methods that operate on a single feature scale, we perform the same cross-scale fusion on the multi-scale features generated by the shared encoder and generate only a single set of initial predictions.

4 Experimental Setup

4.1 Datasets

We perform our experiments on NYUv2 [Nathan Silberman and Fergus, 2012] and Cityscapes [Cordts *et al.*, 2016] datasets, which are both very popular for multitask learning. **NYUv2** contains 1449 densely labelled RGB-depth images of indoor scenes. The raw dataset contains images with incomplete depth values; which are masked during training. The tasks associated with this dataset are 13-label semantic segmentation, depth estimation, and surface normals prediction. The dataset does not contain surface normal labels out-of-the-box, so we used the pseudo ground surface normals data obtained from [Eigen and Fergus, 2015], which include some incomplete values at the same locations as the corresponding depth maps. The training and validation sets contain 795 and 654 images respectively, and the resolution of the images is 288×384 . **Cityscapes** is a larger dataset containing 3475 outdoor urban street scenes with fine annotations taken from 50 cities over several months of the year. From the set of fine annotations, we have 2975 train and 500 validation images. The tasks associated with this dataset are 19-label semantic segmentation and depth estimation. The labels used are from their official documentation that group several labels into a void class, and specify 19 other labels that should be used during training. The resolution of the images is 128×256 .

For both datasets, we use publicly available preprocessed versions courtesy of [Liu *et al.*, 2019].

4.2 Tasks and Performance Metrics

Semantic Segmentation involves assigning a class label to each pixel in an image. During training, the objective is to minimize the depth-wise cross-entropy loss between the predicted labels \hat{y} , and the targets y , for all pixels. We also evaluate our models on mean intersection over union (mIoU) and absolute pixel accuracy. However, mIoU is a much better indicator of semantic understanding.

Depth Estimation involves predicting a depth value for each pixel. During training, we aim to minimize the absolute error (L_1 norm) of the predicted values \hat{d} , and the targets d . We also report on the relative depth error.

Surface Normals prediction involves estimating the direction perpendicular to the surface of objects in an image; making it useful for acquiring geometric and structural scene information. We train the model to minimize the element-wise dot product between the normalized predictions \hat{s} , and the targets s . For evaluation, we consider the mean angular distance

between \hat{s} and s . We also report the proportion of predictions that fall within 11.25, 22.5, and 30.0 degrees of error.

Finally, **MTL Gain** [Maninis *et al.*, 2019] is an aggregate measure of the overall multitask improvement of method m with respect to a single task learning baseline b for all tasks $t \in [1, N]$, as seen in Equation 3.

$$\Delta_m = \frac{1}{N} \sum_t (-1)^{l_t} (M_{m,t} - M_{b,t}) / M_{b,t} \quad (3)$$

where $l_t = 1$ if a lower value of metric M is favorable, and 0 otherwise. We will treat Δ_m as a percentage in our evaluation. Although we use multiple metrics per task throughout our evaluations, we want to make sure that every task is weighed evenly when calculating Δ_m by selecting a single metric per task that best demonstrates generalization performance. Consequently, to compute Δ_m , we will use mIoU for segmentation, the relative error for depth, and the mean angular distance for surface normals. We also show that we still achieve superior MTL gain using other combinations of metrics in the appendix.

In our results, the metrics where larger values are favourable are denoted with (\uparrow) and smaller values with (\downarrow). The formulas for each task-specific performance metric can also be found in the appendix.

4.3 Baselines

It is standard practice in MTL to compare against the traditional STL and MTL baselines. The STL baseline involves using a single network for each task, where each network uses a comparable backbone and output heads as the proposed model for a fair comparison. The MTL baseline uses a hard parameter sharing network [Vandenhende *et al.*, 2022], which involves sharing the backbone layers across all tasks, and then feeding the shared feature representation to each task-specific output head. To make these baselines even more competitive, and to be consistent with the state-of-the-art [Vandenhende *et al.*, 2020], we equip them with a high-resolution network backbone (HRNet18) [Wang *et al.*, 2020] to generate multi-scale features that are processed by scale-specific output heads and aggregated for the final outputs.

Since we are proposing a novel cross-task attention learning mechanism for CNN-based architectures, we must compare with the current best approaches in this domain. Therefore, we will be evaluating against PAD-Net and PAP-Net, which will serve as the EM attention and MM attention baselines, respectively. Additionally, they also serve as our single-scale baselines. Next, we will also compare against MTI-Net, since it is the current state-of-the-art for CNN-based decoder-focused models. This will serve as our multi-scale baseline.

All experiments for our models and the baselines are performed 3 times using a different seed for each experiment. The same set of 3 seeds is used across all models for consistency. The results in all tables contain the average of the converged values across all 3 experiments for each model.

4.4 Implementation Details

Networks: EMA-Net and all baselines are equipped with a pre-trained HRNet18 [Wang *et al.*, 2020] multiscale fea-

Model	NYUv2									Cityscapes		
	Sem. Seg.		Depth		Normals			$\Delta_m \uparrow$	Sem. Seg.	Depth	$\Delta_m \uparrow$	
	mIoU \uparrow	pixAcc \uparrow	relErr \downarrow	mErr \downarrow	mErr \downarrow	11.25 \uparrow	22.5 \uparrow		30 \uparrow	mIoU \uparrow		relErr \downarrow
STL	49.23	72.83	0.1636	0.3853	23.15	35.18	62.50	73.48	+0.00	48.89	29.91	+0.00
MTL	49.25	72.90	0.1658	0.3896	24.16	30.80	57.92	70.41	-1.89	49.78	31.80	-2.25
PAP-Net	50.00	73.25	0.1615	0.3876	23.78	31.90	58.89	71.22	+0.04	50.82	26.97	+6.89
PAD-Net	50.23	73.46	0.1622	0.3814	23.63	32.44	59.51	71.68	+0.27	50.67	27.37	+6.07
EMA-Net (SS)	51.59	74.14	0.1607	0.3808	22.84	35.14	62.06	73.40	+2.64	51.36	23.84	+12.67
MTI-Net	51.51	74.50	0.1538	0.3650	23.50	34.16	60.85	72.31	+3.04	51.77	29.90	+2.96
EMA-Net (MS)	52.70	75.09	0.1529	0.3630	22.99	35.59	62.25	73.28	+4.76	51.94	22.89	+14.85

Table 1: Validation set performance taken across all tasks on NYUv2 and Cityscapes. Values in bold indicate the best value in a given column for multitask models in SS and MS configurations.

ture extractor backbone. The single-scale variants of EMA-Net and the baselines will use a fused version of the input features following the aforementioned CSF procedure. The output heads for the initial predictions include two residual blocks [He *et al.*, 2016] followed by an output convolution layer. The initial predictions used for task-prediction distillation are the outputs of the second residual block. The final output heads for the single-scale models use the same architecture as the heads used for the initial predictions. For multi-scale baselines, we up-sample all outputs to 1/4 input scale, concatenate them along the channel dimension, and process them through a two-layer convolution block to get the final predictions. The implementation code for all baseline networks is taken from [Vandenhende *et al.*, 2020], except for PAP-Net which we implemented ourselves.

Hyper-parameters: We train our models using an Adam [Kingma and Ba, 2014] optimizer with a weight decay of 1×10^{-4} . The learning rates are 1×10^{-4} and 5×10^{-4} for NYUv2 and Cityscapes respectively. We performed a small learning rate search for each model to ensure that this configuration was favourable for all baselines. We also use a cosine annealing learning rate scheduler for smooth convergence. Multi-scale models tend to converge early for Cityscapes, so for them, we used a cosine annealing learning rate scheduler with warm restarts [Loshchilov and Hutter, 2016] to promote exploration and escape local minima. For both datasets, we use a batch size of 8, a blending factor $\gamma = 0.05$ (like PAP-Net) and filter size $f = 3$ for all our models. The values for γ and f were not tuned for each dataset, and our models show little sensitivity to these parameters (see appendix). We train for 200 and 75 epochs on NYUv2 and Cityscapes respectively using a single NVIDIA RTX A5000 GPU.

5 Results

5.1 Ablation Study

To observe the effects of CTAL in our SS and MS configurations, we first evaluate the performance of the base EMA-Net architecture without CTAL or the CSF blocks. Therefore, it only contains a single projection layer for the initial prediction features and the corresponding task-specific decoder heads. Next, we evaluate the performance change from adding CTAL in the single-scale variation, and then with cross-scale fusion in the multi-scale variation. As we can

Model	NYUv2				Cityscapes		
	Sem. Seg.	Depth	Normals	$\Delta_m \uparrow$	Sem. Seg.	Depth	$\Delta_m \uparrow$
	mIoU \uparrow	relErr \downarrow	mErr \downarrow		mIoU \uparrow	relErr \downarrow	
STL	49.23	0.1636	23.15	+0.00	48.89	29.91	+0.00
EMA-Net (Base)	50.01	0.1634	23.65	-0.15	50.33	26.92	+6.47
+CTAL	51.59	0.1607	22.84	+2.64	51.36	23.84	+12.67
+CTAL+CSF	52.70	0.1529	22.99	+4.76	51.94	22.89	+14.85

Table 2: Effectiveness of the different configurations of EMA-Net for both NYUv2 and Cityscapes datasets.

see in Table 2, EMA-Net without CTAL does not outperform the STL baseline for NYUv2 and achieves a +6.47% MTL gain on Cityscapes. Adding CTAL, we can see a +2.64% and +12.67% improvement in the MTL gain for each dataset compared to the STL baseline. Finally, having CTAL with deep supervision at multiple scales with CSF, we see further MTL gains with +4.76% and +14.85% on NYUv2 and Cityscapes respectively. Overall, we see large MTL gains across both datasets using our SS and MS configurations.

5.2 Comparison to State-of-the-Art

Table 1 shows the results of EMA-Net SS and MS against all our baselines. The tables are divided into 3 sections to separate the traditional STL and MTL baselines, the SS models, and the MS models. As we can see, for both datasets, we achieve considerably higher performance for all task metrics in SS and MS configurations. We can even see that our EMA-Net (SS) is competitive to MTI-Net in NYUv2 despite being at a disadvantage by not having deep supervision on task predictions from multiple scales. On Cityscapes, we can also see that MTI-Net struggles in the simpler 2-task setting with smaller input image scales. The results of MTI-Net have likely not been reported previously on Cityscapes as it is susceptible to overfitting. Despite our efforts to mitigate overfitting (i.e. spatial dropout, warm restart scheduler, data augmentation, architectural modifications, hyperparameter tuning), we were unable to achieve better performance than what is seen in Table 1. However, our EMA-Net (MS), which also employs deep supervision on multiscale initial predictions, does not exhibit the same overfitting behaviour. In fact, we further improve performance over EMA-Net (SS).

Since this study targets light-weight CNN-based ap-

proaches, we do not compare with the transformer-based models in this parameter regime. However, we would like to note that when equipped with comparable Transformer backbones, the current CNN-based baselines perform very similarly to the InvPT and TaskPrompter [Ye and Xu, 2023].

5.3 Resource Analysis

As mentioned earlier, the trade-off for using significantly fewer model parameters is that we introduce additional FLOPs. We argue in favor of this trade-off because there are more optimization opportunities at various levels to reduce the effect of additional FLOPs compared to model parameters. For example, we can optimize algorithmically [Fawzi *et al.*, 2022], improve hardware utilization [Kljucaric and George, 2023], leverage sparse matrix operations [Gao *et al.*, 2023] (if applicable), and manipulate feature scales. Table 3 summarizes the resources used for each model on NYUv2 and we can see that we drastically reduce the number of FLOPs by simply reducing the scale at which we perform task prediction distillation. We also see that we can easily reduce the wall clock time to be on par or lower than other methods. We observe that in the SS setting, we outperform PAD-Net with less than half the number of parameters and with even fewer FLOPs. In the MS setting, we use fewer model parameters and still achieve better multitasking performance, even with smaller feature scales.

Model	Scale	Rel Param.	FLOPs	Time (s)	$\Delta_m \uparrow$
MTL	1/4	0.346	42G	2.82	-1.89
PAP-Net	1/4	0.404	521G	17.73	+0.04
PAD-Net	1/4	1.023	484G	6.13	+0.27
EMA-Net (SS)	1/4	0.513	537G	13.85	+2.64
	1/6	0.504	194G	5.97	+1.70
	1/8	0.500	124G	4.37	+1.50
MTI-Net	1/4	1.070	65G	4.45	+3.04
	1/4	0.944	525G	14.26	+4.76
	EMA-Net (MS)	1/6	0.935	190G	6.48
	1/8	0.932	117G	5.23	+3.43

Table 3: Resource analysis of SS and MS models on NYUv2. “Scale” represents the highest feature scale used for task-prediction distillation. “Rel Param.” represents the number of parameters relative to the STL baseline. “FLOPs” represents the number of floating-point operations used in a forward pass. “Time” refers to the wall clock time required to process the entire validation set in seconds. Finally, “ Δ_m ” represents the MTL gain relative to the STL baseline.

Overall, the results demonstrate several efficiency benefits from our proposed method. This can be attributed to how we organize the features to allow for more efficient parameter usage. This also reduces the risk of overfitting, as seen in the results of the Cityscapes dataset. In general, as the trend of using more model capacity for better performance persists, we must be more conscious of how we can optimize efficiency so that these models can be deployed in real-world settings with much stricter memory limitations [Menghani, 2023].

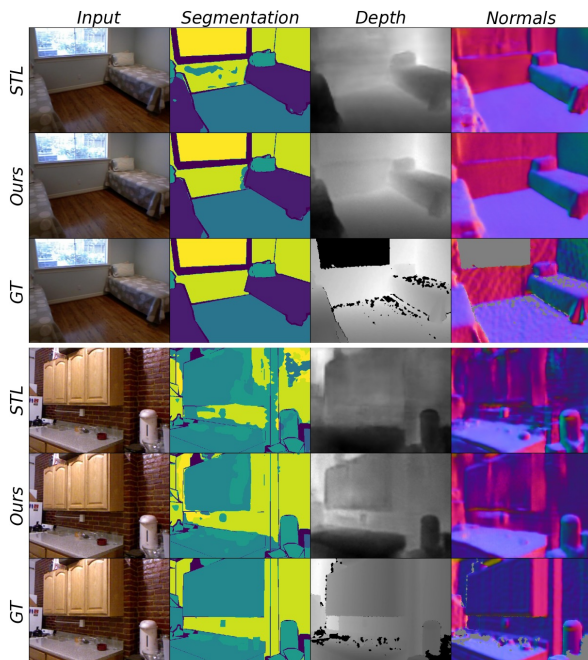


Figure 4: A visual comparison of the predictions from the single task baseline (STL) and EMA-Net (Ours). The two images and the ground truths (GT) are from the validation set of NYUv2.

5.4 Qualitative Analysis

Figure 4 is a visualization of the predictions of our EMA-Net (MS) and the STL baseline on images from the validation set of NYUv2. As we can see, our model produces significantly fewer artifacts in the segmentation maps. Also, our model generates smoother and more granular depth and surface normal maps compared to STL. For instance, we can see our model doesn’t warp structures as much as STL, as seen for the cabinets in the second image. Also, our model generalizes better in undefined regions of the depth and normals tasks, like for the window in the first image.

6 Conclusion

We proposed our EMA-Net multitask architecture, incorporating the novel CTAL module for task prediction distillation. Our network is the first CNN-based architecture that can explicitly and exhaustively model all feature-pair relationships intra- and inter-task. Impressively, we accomplish this using significantly fewer model parameters than competing STL and MTL models while achieving better multitasking performance on complex indoor and outdoor scenes. We have also demonstrated that by adjusting our feature scale, we can significantly reduce the number of FLOPs we introduce while still outperforming competitors at higher feature scales. As mentioned, we believe that the performance improvements with the massive reduction in model parameters justify the additional FLOPs, especially since there are more opportunities for optimization compared to reducing model capacity. Looking ahead, exploring techniques to further mitigate the impact of FLOPs on wall-clock time, such as sparsifying affinity matrices, would be intriguing.

References

- [Brüggemann *et al.*, 2021] David Brüggemann, Menelaos Kanakis, Anton Obukhov, Stamatios Georgoulis, and Luc Van Gool. Exploring relational context for multi-task dense prediction. In *Proceedings of the IEEE/CVF international conference on computer vision*, pages 15869–15878, 2021.
- [Caruana, 1997] Rich Caruana. Multitask learning. *Machine learning*, 28(1):41–75, 1997.
- [Chen *et al.*, 2018] Zhao Chen, Vijay Badrinarayanan, Chen-Yu Lee, and Andrew Rabinovich. Gradnorm: Gradient normalization for adaptive loss balancing in deep multitask networks. In *International conference on machine learning*, pages 794–803. PMLR, 2018.
- [Chollet, 2017] Francois Chollet. Xception: Deep learning with depthwise separable convolutions. In *Proceedings of the IEEE conference on computer vision and pattern recognition*, pages 1251–1258, 2017.
- [Cordts *et al.*, 2016] Marius Cordts, Mohamed Omran, Sebastian Ramos, Timo Rehfeld, Markus Enzweiler, Rodrigo Benenson, Uwe Franke, Stefan Roth, and Bernt Schiele. The cityscapes dataset for semantic urban scene understanding. In *Proc. of the IEEE Conference on Computer Vision and Pattern Recognition (CVPR)*, 2016.
- [Dosovitskiy *et al.*, 2020] Alexey Dosovitskiy, Lucas Beyer, Alexander Kolesnikov, Dirk Weissenborn, Xiaohua Zhai, Thomas Unterthiner, Mostafa Dehghani, Matthias Minderer, Georg Heigold, Sylvain Gelly, et al. An image is worth 16x16 words: Transformers for image recognition at scale. *arXiv preprint arXiv:2010.11929*, 2020.
- [Eigen and Fergus, 2015] David Eigen and Rob Fergus. Predicting depth, surface normals and semantic labels with a common multi-scale convolutional architecture. In *Proceedings of the IEEE international conference on computer vision*, pages 2650–2658, 2015.
- [Fawzi *et al.*, 2022] Alhussein Fawzi, Matej Balog, Aja Huang, Thomas Hubert, Bernardino Romera-Paredes, Mohammadamin Barekatin, Alexander Novikov, Francisco J R Ruiz, Julian Schrittwieser, Grzegorz Swirszcz, et al. Discovering faster matrix multiplication algorithms with reinforcement learning. *Nature*, 610(7930):47–53, 2022.
- [Fu *et al.*, 2019] Jun Fu, Jing Liu, Haijie Tian, Yong Li, Yongjun Bao, Zhiwei Fang, and Hanqing Lu. Dual attention network for scene segmentation. In *Proceedings of the IEEE/CVF conference on computer vision and pattern recognition*, pages 3146–3154, 2019.
- [Gao *et al.*, 2019] Yuan Gao, Jiayi Ma, Mingbo Zhao, Wei Liu, and Alan L Yuille. Nddr-cnn: Layerwise feature fusing in multi-task cnns by neural discriminative dimensionality reduction. In *Proceedings of the IEEE/CVF conference on computer vision and pattern recognition*, pages 3205–3214, 2019.
- [Gao *et al.*, 2023] Jianhua Gao, Weixing Ji, Fangli Chang, Shiyu Han, Bingxin Wei, Zeming Liu, and Yizhuo Wang. A systematic survey of general sparse matrix-matrix multiplication. *ACM Computing Surveys*, 55(12):1–36, 2023.
- [He *et al.*, 2016] Kaiming He, Xiangyu Zhang, Shaoqing Ren, and Jian Sun. Deep residual learning for image recognition. In *Proceedings of the IEEE conference on computer vision and pattern recognition*, pages 770–778, 2016.
- [Kendall *et al.*, 2018] Alex Kendall, Yarin Gal, and Roberto Cipolla. Multi-task learning using uncertainty to weigh losses for scene geometry and semantics. In *Proceedings of the IEEE conference on computer vision and pattern recognition*, pages 7482–7491, 2018.
- [Kingma and Ba, 2014] Diederik P Kingma and Jimmy Ba. Adam: A method for stochastic optimization. *arXiv preprint arXiv:1412.6980*, 2014.
- [Kljucaric and George, 2023] Luke Kljucaric and Alan D George. Deep learning inferring with high-performance hardware accelerators. *ACM Transactions on Intelligent Systems and Technology*, 14(4):1–25, 2023.
- [Liu *et al.*, 2019] Shikun Liu, Edward Johns, and Andrew J Davison. End-to-end multi-task learning with attention. In *Proceedings of the IEEE/CVF conference on computer vision and pattern recognition*, pages 1871–1880, 2019.
- [Liu *et al.*, 2022] Shikun Liu, Stephen James, Andrew J Davison, and Edward Johns. Auto-lambda: Disentangling dynamic task relationships. *arXiv preprint arXiv:2202.03091*, 2022.
- [Loshchilov and Hutter, 2016] Ilya Loshchilov and Frank Hutter. Sgdr: Stochastic gradient descent with warm restarts. *arXiv preprint arXiv:1608.03983*, 2016.
- [Maninis *et al.*, 2019] Kevis-Kokitsi Maninis, Ilija Radosavovic, and Iasonas Kokkinos. Attentive single-tasking of multiple tasks. In *Proceedings of the IEEE/CVF conference on computer vision and pattern recognition*, pages 1851–1860, 2019.
- [Menghani, 2023] Gaurav Menghani. Efficient deep learning: A survey on making deep learning models smaller, faster, and better. *ACM Computing Surveys*, 55(12):1–37, 2023.
- [Misra *et al.*, 2016] Ishan Misra, Abhinav Shrivastava, Abhinav Gupta, and Martial Hebert. Cross-stitch networks for multi-task learning. In *Proceedings of the IEEE conference on computer vision and pattern recognition*, pages 3994–4003, 2016.
- [Nathan Silberman and Fergus, 2012] Pushmeet Kohli Nathan Silberman, Derek Hoiem and Rob Fergus. Indoor segmentation and support inference from rgbd images. In *ECCV*, 2012.
- [Sandler *et al.*, 2018] Mark Sandler, Andrew Howard, Menglong Zhu, Andrey Zhmoginov, and Liang-Chieh Chen. Mobilenetv2: Inverted residuals and linear bottlenecks. In *Proceedings of the IEEE conference on computer vision and pattern recognition*, pages 4510–4520, 2018.
- [Sinodinos and Armanfard, 2022] Dimitrios Sinodinos and Narges Armanfard. Attentive task interaction network for multi-task learning. In *2022 26th International Conference on Pattern Recognition (ICPR)*, pages 2885–2891. IEEE, 2022.

- [Vandenhende *et al.*, 2020] Simon Vandenhende, Stamatios Georgoulis, and Luc Van Gool. Mti-net: Multi-scale task interaction networks for multi-task learning. In *Computer Vision–ECCV 2020: 16th European Conference, Glasgow, UK, August 23–28, 2020, Proceedings, Part IV 16*, pages 527–543. Springer, 2020.
- [Vandenhende *et al.*, 2022] Simon Vandenhende, Stamatios Georgoulis, Wouter Van Gansbeke, Marc Proesmans, Dengxin Dai, and Luc Van Gool. Multi-task learning for dense prediction tasks: A survey. *IEEE Transactions on Pattern Analysis and Machine Intelligence*, 44(7):3614–3633, 2022.
- [Vaswani *et al.*, 2017] Ashish Vaswani, Noam Shazeer, Niki Parmar, Jakob Uszkoreit, Llion Jones, Aidan N Gomez, Łukasz Kaiser, and Illia Polosukhin. Attention is all you need. *Advances in neural information processing systems*, 30, 2017.
- [Wang *et al.*, 2020] Jingdong Wang, Ke Sun, Tianheng Cheng, Borui Jiang, Chaorui Deng, Yang Zhao, Dong Liu, Yadong Mu, Mingkui Tan, Xinggang Wang, et al. Deep high-resolution representation learning for visual recognition. *IEEE transactions on pattern analysis and machine intelligence*, 43(10):3349–3364, 2020.
- [Woo *et al.*, 2018] Sanghyun Woo, Jongchan Park, Joon-Young Lee, and In So Kweon. Cbam: Convolutional block attention module. In *Proceedings of the European conference on computer vision (ECCV)*, pages 3–19, 2018.
- [Xie *et al.*, 2017] Saining Xie, Ross Girshick, Piotr Dollár, Zhuowen Tu, and Kaiming He. Aggregated residual transformations for deep neural networks. In *Proceedings of the IEEE conference on computer vision and pattern recognition*, pages 1492–1500, 2017.
- [Xin *et al.*, 2022] Derrick Xin, Behrooz Ghorbani, Justin Gilmer, Ankush Garg, and Orhan Firat. Do current multi-task optimization methods in deep learning even help? *Advances in Neural Information Processing Systems*, 35:13597–13609, 2022.
- [Xu *et al.*, 2018] Dan Xu, Wanli Ouyang, Xiaogang Wang, and Nicu Sebe. Pad-net: Multi-tasks guided prediction-and-distillation network for simultaneous depth estimation and scene parsing. In *Proceedings of the IEEE Conference on Computer Vision and Pattern Recognition*, pages 675–684, 2018.
- [Ye and Xu, 2022] Hanrong Ye and Dan Xu. Inverted pyramid multi-task transformer for dense scene understanding. In *ECCV*, 2022.
- [Ye and Xu, 2023] Hanrong Ye and Dan Xu. Taskprompter: Spatial-channel multi-task prompting for dense scene understanding. In *ICLR*, 2023.
- [Zhang *et al.*, 2019] Zhenyu Zhang, Zhen Cui, Chunyan Xu, Yan Yan, Nicu Sebe, and Jian Yang. Pattern-affinitive propagation across depth, surface normal and semantic segmentation. In *Proceedings of the IEEE/CVF conference on computer vision and pattern recognition*, pages 4106–4115, 2019.